

Non-Franck-Condon electron-impact dissociative-excitation cross sections of molecular hydrogen producing $H(1s) + H(2l)$ through $X^1\Sigma_g^+(v=0) \rightarrow \{B^1\Sigma_u^+, B'^1\Sigma_u^+, C^1\Pi_u\}$

Itamar Borges, Jr.,¹ Ginette Jalbert,¹ and Carlos Eduardo Bielschowsky²

¹*Instituto de Física, Departamento de Física Nuclear, Universidade Federal do Rio de Janeiro, Cidade Universitária, CT Bloco A, Caixa Postal 68528, Rio de Janeiro, 21945-970, Rio de Janeiro, Brazil*

²*Instituto de Química, Departamento de Físico-Química, Universidade Federal do Rio de Janeiro, Cidade Universitária, CT Bloco A, Rio de Janeiro, 21949-900, Rio de Janeiro, Brazil*

(Received 21 August 1997)

Dissociation cross sections of H_2 for high-energy electron impact (100–1000 eV) producing $H(1s)$, $H(2s)$, and $H(2p)$ for excitation from the ground vibrational state ($v=0$) to the continuum of the $B^1\Sigma_u^+$, $B'^1\Sigma_u^+$, and $C^1\Pi_u$ states were computed in the first Born approximation. Configuration-interaction electronic wave functions were used and vibrational degrees of freedom taken in account. The dissociative excitation cross sections as a function of the continuum energy for each final state were presented, and the accuracy of the wave function, including the importance of relaxation effects and the validity of the Franck-Condon approximation, is analyzed in comparison to available previous theoretical results. The computed dissociation cross sections were compared to experimental results making use of the separation of the various breakup channels proposed by Ajello, Shemansky, and James [Astrophys. J. **371**, 422 (1991)]. The obtained cross sections to produce $H(2p) + H(1s)$ fragments via dissociative excitation to the B and C states have agreed well with the decomposed experimental results within the error bars. The dissociation cross sections to produce $H(2s) + H(1s)$ through the B' state were in most cases somewhat larger than the reported experimental error bars. In the most favorable case our theoretical B' dissociation cross section was 3.1% within the reported error bar at 300 eV electron impact energy. A possible experimental reason for this discrepancy was raised.

[S1050-2947(98)01502-9]

PACS number(s): 34.80.Ht

I. INTRODUCTION

Investigations of collision processes involving atoms and molecules with electrons, atoms, and molecules are still being performed extensively both experimentally and theoretically. Among the recent interests, it is worth mentioning high-energy molecular destruction of simple diatomic molecules H_2 , H_2^+ , HeH^+ interacting with noble gases over a wide range of energy [1], electron- [2–4], and photon- [5] impact dissociation cross sections.

Collision processes involving electron impact on hydrogen molecules are of most fundamental relevance in the study of electron-molecule collisions. A compilation of these cross sections for various collision channels can be found in Tawara *et al.* [2]. Accurate knowledge of electron-impact dissociation cross sections is important for modeling of plasmas, interstellar matter, correct estimation of predissociation yields, etc. Experimental measurements of dissociation cross sections are done indirectly by detecting radiation emitted by the excited atomic fragments, making them very difficult to perform [3,6,7]. As the estimation of each channel involved in the experimental determination of the breaking of a molecule depends on available theoretical cross sections, *ab initio* theoretical methods are claimed [3] in the interpretation and analysis of the experimental data.

As part of an ongoing project of calculation of high-energy electron-impact dissociative cross sections of diatomic molecules we report data for H_2 . Despite being the simplest dissociation process, only a few theoretical calculations of high-energy electron-impact dissociative-excitation

cross sections from the ground state $X^1\Sigma_g^+(v=0)$ for H_2 [4,8–11] have been done. Among them, there are calculations for transitions to the $B'^1\Sigma_u^+$ state [4,8–10] and to the $B^1\Sigma_u^+$ and $C^1\Pi_u$ states [11]. The work of Lee *et al.* [9] uses the distorted-wave approximation and involved impact energies only up to 100 eV, Chung *et al.* [8] consider energies up to 1000 eV in the Born and Born-Ochkur theories, calculations of Celiberto *et al.* [11] cover a limited range of electron-impact energies (up to 250 eV) in the framework of parameter impact theory, and Liu and Hagstrom [4] use the Bethe approximation valid only at very high projectile energies. All these calculations assume a frozen-core description; i.e., the same set of molecular orbitals is utilized to describe both the ground and excited states.

Here we report *ab initio* adiabatic theoretical calculations of cross sections of electron-impact dissociative-excitation cross sections for producing $H(1s) + H(2s)$ through the $X^1\Sigma_g^+(v=0) \rightarrow B'^1\Sigma_u^+$ transition and producing $H(1s) + H(2p)$ through the $X^1\Sigma_g^+(v=0) \rightarrow \{B^1\Sigma_u^+, C^1\Pi_u\}$ transitions in the framework of the first Born approximation. We also present the dissociation cross sections as a function of the continuum energy. The methodology used here is an extension of the one already developed for inner-shell [12,13,15] and valence electronic excitation processes [14,16], and goes further as it describes dissociation, including the vibrational degrees of freedom. We have used configuration interaction (CI) for the target electronic wave functions, which takes into account both correlation and relaxation effects. In particular, we have investigated relaxation effects in the dipole transition moment. The validity of

the Franck-Condon approximation has also been investigated. The calculated cross sections are compared to previous theoretical [4,8–11] values and to the available experiments [3,6,7]. For the latter the separation of the various breakup channels proposed by Ajello, Shemansky, and James is used [3].

II. THEORETICAL BACKGROUND

A. Dissociation cross section in the first Born approximation

We are concerned with the process where a hydrogen molecule, when excited by electron impact to the vibrational continuum levels of a bound state, dissociates in a ground-state atom $H(1s)$ and an excited one [$H(2s)$ or $H(2p)$]. Concerning these fragments, two distinct groups of energy distributions are formed on dissociative excitation of H_2 : the “fast” and “slow” groups [3]. The slow $H(2s)$ atoms arise from a transition to singly excited states above the $H(1s) + H(2s)$ dissociation limit and likewise for the $H(2p)$ atoms. Of all possible singly excited molecular states, we are interested in the $B^1\Sigma_u^+$ and $C^1\Pi_u$ states, producing adiabatically $H(2p)$, and $B'^1\Sigma_u^+$, producing adiabatically $H(2s)$. Contributions from double excited states, which produce fast fragments [3], are not considered. Dissociation can also take place by excitation to a purely repulsive electronic state or through predissociation [17]; these processes are also not considered here. The rotational motion of the molecule is taken into account by summing over the final rotational states accessible energetically and by averaging the initial rotational states [18]. Atomic units are used throughout.

According to the Born-Oppenheimer approximation, we may write the wave functions of the ground electronic-vibrational (00) state and of the final state (nW) as

$$\Psi_{00}(\mathbf{r}_1, \mathbf{r}_2, \mathbf{R}) = \psi_0(\mathbf{r}_1, \mathbf{r}_2, \mathbf{R})\chi_{00}(R), \quad (1)$$

$$\Psi_{nW}(\mathbf{r}_1, \mathbf{r}_2, \mathbf{R}) = \psi_n(\mathbf{r}_1, \mathbf{r}_2, \mathbf{R})\chi_{nW}(R), \quad (2)$$

where \mathbf{r}_1 and \mathbf{r}_2 are the electron coordinates of H_2 , \mathbf{R} the internuclear distance, ψ_0 and ψ_n are the electronic wave functions of the ground (0) and excited (n) states, $\chi_{00}(R)$ is the discrete ($v=0$) vibrational function of the ground state, and $\chi_{nW}(R)$ is the unbound vibrational function of the final state defined by the corresponding energy W above the dissociation limit ($R \rightarrow \infty$) [8]. The electronic wave functions ψ_0 and ψ_n , constructed at the configuration-interaction level, will be discussed in detail in the next section. The spin functions are factored out in Eqs. (1) and (2) since we do not consider spin-orbit interactions.

The collision process is characterized by the wave vectors of the incident and scattered electron, \mathbf{k}_{00} and \mathbf{k}_{nW} , \mathbf{K} being the transferred momentum $\mathbf{k}_{00} - \mathbf{k}_{nW}$. We define the electronic transition amplitude in the first Born approximation [8,18,19] as

$$\begin{aligned} \varepsilon_{0n}(K, R, \Theta, \Phi) &= \varepsilon_{0n}(K, R, \Omega) \\ &= - \int \psi_n^*(\mathbf{r}_1, \mathbf{r}_2, \mathbf{R}) \left(\sum_{i=1}^N e^{i\mathbf{K} \cdot \mathbf{r}_i} \right) \\ &\quad \times \psi_0(\mathbf{r}_1, \mathbf{r}_2, \mathbf{R}) d\mathbf{r}_1 d\mathbf{r}_2, \end{aligned} \quad (3)$$

TABLE I. Vertical transition energies. See text for discussion.

| Final states | ΔE (eV) | | |
|------------------|-----------------|---------------------|---------------------------|
| | Present | Theoretical [22,23] | Experimental ^a |
| $B^1\Sigma_u^+$ | 12.81 | 12.75 | 12.75 |
| $B'^1\Sigma_u^+$ | 14.83 | 14.85 | 14.85 |
| $C^1\Pi_u$ | 13.22 | 13.22 | 13.29 |

^aCited by Sabin and Oddershed [26].

where Θ and Φ ($\equiv \Omega$) specify the relative orientation between \mathbf{R} and \mathbf{K} ; N is the molecule electron number—equal to 2 for molecular hydrogen. The electronic transition amplitude $\varepsilon_{0n}(K, R, \Omega)$ was calculated in the internuclear distance interval $1.0 \leq R \leq 2.4$ a.u. in steps of 0.2 a.u. Similar to the excitation of discrete vibrational levels [18,19], the differential cross sections for excitation to a unit energy range about W above the dissociation limit of the final state are given by [8]

$$\begin{aligned} \left(\frac{d\sigma}{d\omega dW} \right)_n &= \frac{g_n}{4\pi} \frac{k_{nW}}{k_{00}} \\ &\quad \times \int \left| \int \chi_{nW}^*(R)\chi_{00}(R)\varepsilon_{0n}(K, R, \Omega) dR \right|^2 d\Omega, \end{aligned} \quad (4)$$

where g_n is the degeneracy of the final state (1 for Σ , 2 for Π), and $\omega = (\theta, \phi)$ is the scattered angle of the projectile electron, which is directly related to the transferred momentum \mathbf{K} [$d\omega = 2\pi \sin\theta d\theta = 2\pi K dK / (k_{00}k_{nW})$]. The integration over Ω results from averaging over the orientation of the molecular axis with respect to \mathbf{K} , as mentioned before. Integration of the differential cross section over K (or ω) from K_{\min} ($=k_{00} - k_{nW}$) to K_{\max} ($=k_{00} + k_{nW}$) [18] gives the differential dissociation cross section $d\sigma/dW$ of excitation over a unit range about W of the final state

$$\left(\frac{d\sigma}{dW} \right)_n = \int \frac{d\sigma}{d\omega dW} d\omega. \quad (5)$$

It is important to emphasize that the greatest contribution to the dissociation cross sections comes from the small transferred momenta [18].

Finally, the total dissociation cross section through excitation to the continuum of an electronic state is

$$\sigma_n = \int_0^\infty \left(\frac{d\sigma}{dW} \right)_n dW. \quad (6)$$

The upper limit (∞) is for all practical purposes taken when $d\sigma/dW$ has decreased several orders of magnitude.

Our calculations are not based on the Franck-Condon principle; however, it is interesting to check the validity of this approximation. Within this approximation, Eq. (4) is simplified, eliminating the R dependence of ε_{0n} ,

$$\left(\frac{d\sigma}{d\omega dW} \right)_n \approx \frac{g_n}{4\pi} \frac{k_{nW}}{k_{00}} q_{nW} \int |\varepsilon_{0n}(K, R_0, \Omega)|^2 d\Omega, \quad (7)$$

TABLE II. Dipole transition moments— $B \ ^1\Sigma_u^+$.

| R (a.u.) | Present CI-R | Wolniewicz [28] |
|------------|--------------|---------------------|
| 1.0 | 0.7269 | 0.7650 |
| 1.2 | 0.8359 | 0.8708 |
| 1.4 | 0.9236 | 0.9821 ^a |
| 1.6 | 1.025 | 1.096 |
| 1.8 | 1.125 | 1.208 |
| 2.0 | 1.218 | 1.313 |
| 2.2 | 1.302 | 1.408 |
| 2.4 | 1.372 | 1.487 |

^aCeliberto and Rescigno [31] report 0.9821 for this distance.

where R_0 is taken as the equilibrium bond length of the ground state, equal to 1.4 a.u. for H_2 , and q_{nW} is the Franck-Condon factor,

$$q_{nW} = \left| \int \chi_{nW}^*(R) \chi_{00}(R) dR \right|^2. \quad (8)$$

For the purpose of evaluating the quality of our electronic wave functions we define the electronic dipole transition moment in the length form [18] as

$$M_{0n}(R) = - \int \psi_n^*(\mathbf{r}_1, \mathbf{r}_2, \mathbf{R}) \left(\sum_{i=1}^2 x_i \right) \psi_0(\mathbf{r}_1, \mathbf{r}_2, \mathbf{R}) d\mathbf{r}_1 d\mathbf{r}_2, \quad (9)$$

where x_i is a component of \mathbf{r}_i , the electron coordinate. The effect of the electron exchange was not considered in the computation of the dissociation cross sections once it is known to be unimportant [4,20] for high-energy electron-impact energies, as was investigated by Chung and Lin for electron excitation of $B \ ^1\Sigma_u^+$ of H_2 at 100 eV [20].

B. Target wave functions

Discrete ($v=0$) and continuum vibrational wave functions were obtained by integrating numerically the nuclear Schrödinger equation, according to Le Roy's methodology [21], from the most accurate potential curves available [22,23]. The purpose was to obtain the most accurate vibrational wave functions. The Born-Oppenheimer energies are taken from Ref. [22] for the ground state (X) and from Ref. [23] for the excited states (B, B', C). We have also used Le Roy's program to perform the R integration of Eq. (4).

Electronic wave functions were obtained within the distance interval $1.0 \leq R \leq 2.4$ a.u. (steps of 0.2 a.u.) at the configuration-interaction level with single and double excitations (CI-SD) expanded on a basis of Gaussian-type orbitals. After several tests we have chosen the basis $(12s, 6p, 3d)/[9s, 6p, 3d]$ suggested by Jaszunski and Roos [24].

Two different types of CI calculations were performed to obtain the electronic state wave functions. In the first one the frozen-core model was assumed (CI-FC); i.e., the same set of molecular orbitals (MOs), occupied and virtual, described the ground and the excited states. In the second one we solved self-consistently for the excited-state wave functions, allowing all the molecular orbitals to fully relax (CI-R). For the latter case an implemented biorthogonalization procedure allows us to compute matrix elements $\varepsilon_{0n}(K, R, \Omega)$ [Eq. (3)] between the wave functions built up from nonorthogonal atomic or molecular orbitals [15].

The MOs used for the CI relaxed (CI-R) calculations were constructed from the Hartree-Fock occupied molecular orbitals of the lowest symmetry and a virtual space of improved virtual orbitals (IVOs) of Hunt and Goddard [25]. The full CI space of 48 MOs (occupied plus virtual) was made of $10\sigma_g$, $10\sigma_u$, $12\pi_u$, $12\pi_g$, and 4δ MOs. For the $X \ ^1\Sigma_g^+$ and $C \ ^1\Pi_u$ states the occupied and the virtual MOs utilized to generate the IVOs were constructed from the respective Hartree-Fock molecular orbitals. For the $B \ ^1\Sigma_u^+$ and $B' \ ^1\Sigma_u^+$ states the occupied MOs and the virtual space with the IVOs was constructed from the first Hartree-Fock excited-state MOs of Σ_u^+ symmetry, the $B \ ^1\Sigma_u^+$ state. Concerning the CI frozen core (CI-FC) calculation the $X \ ^1\Sigma_g^+$ MOs and the corresponding IVO set were utilized both for the ground and the excited states. For the relaxed and frozen-core wave functions all single and double excitations were allowed from the reference configurations, the single electronic configuration of the lowest symmetry for each state.

III. CALCULATED RESULTS AND DISCUSSIONS

A. Wave functions and transition moments

The ground-state energy obtained (at the internuclear equilibrium distance $R=1.4$ a.u.) was 1.171 368 a.u., which can be compared to the 1.174 476 a.u. of Kolos *et al.* [22]. A measure on the balancing of the electronic wave functions, an important condition to compute accurate transition matrix elements, is to compare the theoretical vertical excitation en-

TABLE III. Dipole transition moments— $B' \ ^1\Sigma_u^+$.

| R (a.u.) | Present CI-R | Wolniewicz [28] | Liu and Hagstrom [4] | Ford <i>et al.</i> [30] ^a |
|------------|--------------|-----------------|----------------------|--------------------------------------|
| 1.0 | 0.3262 | | | 0.3306 |
| 1.2 | 0.3584 | | | 0.3698 |
| 1.4 | 0.3886 | 0.3966 | 0.3976 | 0.3992 |
| 1.6 | 0.4148 | | | 0.4218 |
| 1.8 | 0.4352 | 0.4355 | 0.4334 | 0.4411 |
| 2.0 | 0.4478 | 0.4388 | 0.4365 | 0.4411 |
| 2.2 | 0.4503 | 0.4294 | 0.4269 | |
| 2.4 | 0.4407 | | | |

^aDipole transition moments in the length form.

TABLE IV. Dipole transition moments— $C^1\Pi_u$.

| R (a.u.) | Present CI-R | Wolniewicz [29] |
|------------|--------------|---------------------|
| 1.0 | 0.6443 | 0.6460 |
| 1.2 | 0.6944 | 0.6961 |
| 1.4 | 0.7421 | 0.7433 |
| 1.6 | 0.7872 | 0.7871 |
| 1.8 | 0.8290 | 0.8272 |
| 2.0 | 0.8672 | 0.8634 ^a |
| 2.2 | 0.9012 | 0.8952 |
| 2.4 | 0.9308 | 0.9225 |

^aCeliberto and Rescigno [31] report 0.8460 for this distance.

ergies with the experimental values. This is done at Table I with our excitation energies obtained with the CI-R calculation. We have verified that the CI-FC excitation energies are identical. The explanation for the latter in the molecular hydrogen is that the virtual space built from the ground-state improved virtual orbitals is sufficient to account for relaxation effects in the excitation energy of Rydberg and valence states. Relaxation effects may also be indirectly recovered by CI calculations as already verified in the past for atoms [13] and molecules [15,25].

There is good overall agreement among our vertical excitation energies, the accurate theoretical ones [22,23], and the experimental values cited in [26]. At the other distances in the interval $1.0 \leq R \leq 2.4$ a.u. the comparison of our excitation energies with the accurate theoretical values [22,23] showed differences not greater than 0.03 eV for the three states, except for the distances 2.2 and 2.4 a.u., well outside the Franck-Condon region (interval ~ 1.2 – 1.8 a.u.), where the differences reached 0.3 eV for the $B^1\Sigma_u^+$.

Another way to investigate the quality of the electronic wave function is to compare our computed electronic dipole transition moment, in the length form, with available theoretical results for the $B'^1\Sigma_u^+$ states [4,28,30] and for $B^1\Sigma_u^+$ [27] and $C^1\Pi_u$ states [29]. These previous results, except the ones of Wolniewicz *et al.* [27–29], were obtained in the frozen-core approximation. The results of Wolniewicz *et al.* are considered “exact.” In Tables II–IV we present our CI-R dipole transition moments for the three states and the scarce available theoretical results. The CI-FC results are not presented as they are identical to the CI-R ones. This is not always true for other systems as was shown previously [12–16]. Let us define an average percent difference as $(M_{\text{Wol}} - M_{\text{ours}}) / [(M_{\text{Wol}} + M_{\text{ours}}) / 2]$, from our electronic dipole transition moments M_{ours} to the “exact” results M_{Wol} [28,29]. Looking at Tables II–IV one sees a good agreement between our dipole transition moments and the exact results [27–29], the worst results being the $B^1\Sigma_u^+$ state, although the average difference does not exceed 7.8% at $R = 2.2$ a.u. As the corresponding $B^1\Sigma_u^+$ dissociation cross sections (Table V) have the lower values when compared to the $C^1\Pi_u$ results, the effect of this error on the comparison with the experimental results is negligible. The $B'^1\Sigma_u^+$ and $C^1\Pi_u$ states present better agreement than the $B^1\Sigma_u^+$ state when compared to the “exact” and other results.

A sample of the general behavior of electronic transition amplitude in the first Born approximation as a function of the

TABLE V. Total dissociation cross sections for the transition $X^1\Sigma_g^+ \rightarrow B^1\Sigma_u^+$.

| E_{imp} (eV) | σ_{diss} (10^{-18} cm ²) Present results |
|-----------------------|--|
| 100 | 0.160 |
| 200 | 0.108 |
| 300 | 0.0843 |
| 400 | 0.0686 |
| 500 | 0.0591 |
| 800 | 0.0485 |
| 1000 | 0.0347 |

internuclear distance R (Ω and K fixed), Eq. (3), may be seen in Figs. 1(a)–1(c) for the three transitions. Within the distance interval $1.0 \leq R \leq 2.4$ a.u. the electronic transition amplitude is accurately described by a second-order polynomial [32].

B. Theoretical dissociation cross sections

The computed dissociation cross sections, together with the available theoretical results, for each transition, are presented at Tables V–VII. Figures 2(a)–2(c) depict the cross sections for the three dissociative transitions as a function of the continuum energy for 1000 eV electron-impact energy. The behavior of dissociation cross sections, as a function of the continuum energy, is similar for all calculated electron-impact energies between 100 and 1000 eV.

Our calculations do not include the nonadiabatic (i.e., non-Born-Oppenheimer) interaction that couples the B and B' at large internuclear distances ($\sim 15a_0$) [33]. They must be taken into account when the branching ratio of the production of $H(2p)$ to $H(2s)$ fragments is evaluated. Nonadiabatic effects also cause oscillations on the B and B' states' photodissociation cross sections as a function of the continuum energy as verified by Beswick and Glass-Maujean [33]. On the other hand, the total photodissociation cross section ($B + B'$ states) does not change significantly from those calculated without including the nonadiabatic couplings [33,34], as they have been compared favorably with experiments [35]. We expect the same behavior concerning our electron dissociation cross sections and possible future electron-impact experiments involving H_2 .

Our dissociation cross sections as a function of the continuum energy [Figs. 2(a)–2(c)] have similar threshold behavior when compared to the adiabatic photodissociation cross sections calculations of Glass-Maujean [35]. This is due to the expected identical behavior (in the Franck-Condon region) of the electronic transition amplitude at small K transferred momentum, Eq. (3), and the dipole transition moment, Eq. (9), both quadratic as a function of the internuclear distance, and to the similar discrete and continuum vibrational wave functions obtained from identical potential-energy curves. In particular, the dissociation cross section for the $C^1\Pi_u$ state is negligible at threshold [Fig. 2(c)] and increases, reaching a maximum for energies of about 200 cm^{-1} . The reason is that the $C^1\Pi_u$ state is known to present a potential hump [36] and the cross section peaks when the

TABLE VI. Total dissociation cross sections for the transition $X^1\Sigma_g^+ \rightarrow B'^1\Sigma_u^+$.

| E_{imp} (eV) | σ_{diss} (10^{-18} cm 2) | | | | |
|-----------------------|---|---------------------------|----------------------|-----------------------|-------------------------|
| | Present | Redmon <i>et al.</i> [10] | Liu and Hagstrom [4] | Lee <i>et al.</i> [9] | Chung <i>et al.</i> [8] |
| 100 | 2.34 | 2.88 | 3.06 | 3.41 | 3.09 |
| 200 | 1.54 | 1.99 | 2.05 | | 2.10 |
| 300 | 1.16 | 1.54 | 1.57 | | |
| 400 | 0.946 | | 1.29 | | |
| 500 | 0.802 | | 1.10 | | 1.13 |
| 800 | 0.562 | | 0.777 | | |
| 1000 | 0.473 | | 0.655 | | 0.674 |

transferred energy by the projectile electron reaches the potential-energy maximum.

We have checked the validity of the Franck-Condon approximation, Eq. (7). All the corresponding cross sections were bigger than the ones not using the Franck-Condon approximation, in accordance with previous theoretical results [10,11]. The *ratio* of the Franck-Condon cross sections, Eq. (7), to the non-Franck-Condon cross sections, Eq. (4), for the transitions to the $B^1\Sigma_u^+$, $B'^1\Sigma_u^+$, and $C^1\Pi_u$ states were, respectively, 1.741, 1.07, and 1.236. It is seen that the Franck-Condon approximation may be an unrealistic approximation for the cross-section calculations, especially for the transition to the $B^1\Sigma_u^+$ and $C^1\Pi_u$ states.

The theoretical total dissociation cross sections computed [Eq. (6)] for the transition $X^1\Sigma_g^+(v=0) \rightarrow B^1\Sigma_u^+$ are in Table V. The other available theoretical cross sections were estimated from Fig. 1 of Celiberto *et al.* [11]. Celiberto *et al.*'s estimated dissociation cross sections were 0.16×10^{-18} and 0.11×10^{-18} cm 2 at electron-impact energies of 100 and 200 eV, respectively. Very good agreement was thus obtained between our results and their impact-parameter calculations [11], which uses its own computed electronic dipole transition moment.

Concerning the transition $X^1\Sigma_g^+(v=0) \rightarrow C^1\Pi_u$, our dissociation cross sections are shown in Table VII. Celiberto *et al.*'s [11] cross sections for the same transition were estimated from their Fig. 2. The estimated dissociation cross sections [11] were 0.46×10^{-18} cm 2 (100 eV) and 0.32×10^{-18} cm 2 (200 eV), in very good agreement with our results, such as the $X^1\Sigma_g^+(v=0) \rightarrow B^1\Sigma_u^+$ transition.

The theoretical total dissociation cross sections for the transition $X^1\Sigma_g^+(v=0) \rightarrow B'^1\Sigma_u^+$ are in Table VI, where

TABLE VII. Total dissociation cross sections for the transition $X^1\Sigma_g^+ \rightarrow C^1\Pi_u$.

| E_{imp} (eV) | σ_{diss} (10^{-18} cm 2) |
|-----------------------|---|
| | Present results |
| 100 | 0.466 |
| 200 | 0.317 |
| 300 | 0.245 |
| 400 | 0.201 |
| 500 | 0.171 |
| 800 | 0.121 |
| 1000 | 0.103 |

other available theoretical results have been reported. The present results are lower than the other ones, and an analysis of this discrepancy follows.

The results of Redmon *et al.* [10] employ an impact-parameter formulation, using the calculated electronic dipole transition moments of Ford *et al.* [30] and an approximate potential curve for the B' state [37]. Table VI shows an average difference from our results ranging from 22% (100 eV) to 29% (300 eV). The difference does not seem to be related to the different theoretical approximations, as the impact-parameter formulation was also used by Celiberto *et al.* [11] for the $X^1\Sigma_g^+(v=0) \rightarrow B^1\Sigma_u^+$ and $X^1\Sigma_g^+(v=0) \rightarrow C^1\Pi_u$ dissociation channels, and a very good agreement with our results was obtained, as discussed above. This discrepancy does not seem to be related to the dipole matrix elements either as Table III shows an agreement between our dipole transition moments and the values used by Redmon *et al.* [10] (from Ford *et al.* [30]), in the worst case ($R = 1.2$ a.u.) having an average difference from Ford *et al.*'s of 3.1%. It might be related to the vibrational wave functions used in Redmon *et al.*'s [10] work, although Liu and Hagstrom [4] checked that an error of only 8% may arise from computing dissociation cross sections for this transition using approximate vibrational wave functions from Spindler's [37] B' experimental potential curve.

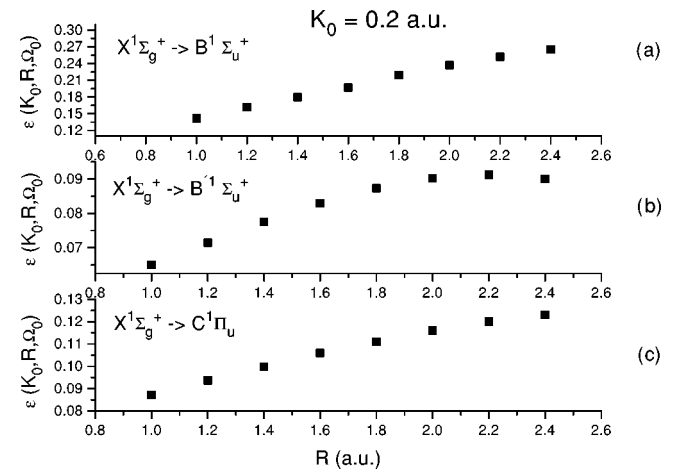


FIG. 1. General behavior of electronic transition amplitude in the first Born approximation as a function of the internuclear distance R for $K = 0.2$ a.u. and fixed $\Omega = \Omega_0$ [Eq. (3)] for the (a) $X^1\Sigma_g^+(v=0) \rightarrow B^1\Sigma_u^+$, (b) $X^1\Sigma_g^+(v=0) \rightarrow B'^1\Sigma_u^+$, and (c) $X^1\Sigma_g^+ \rightarrow C^1\Pi_u$ transitions.

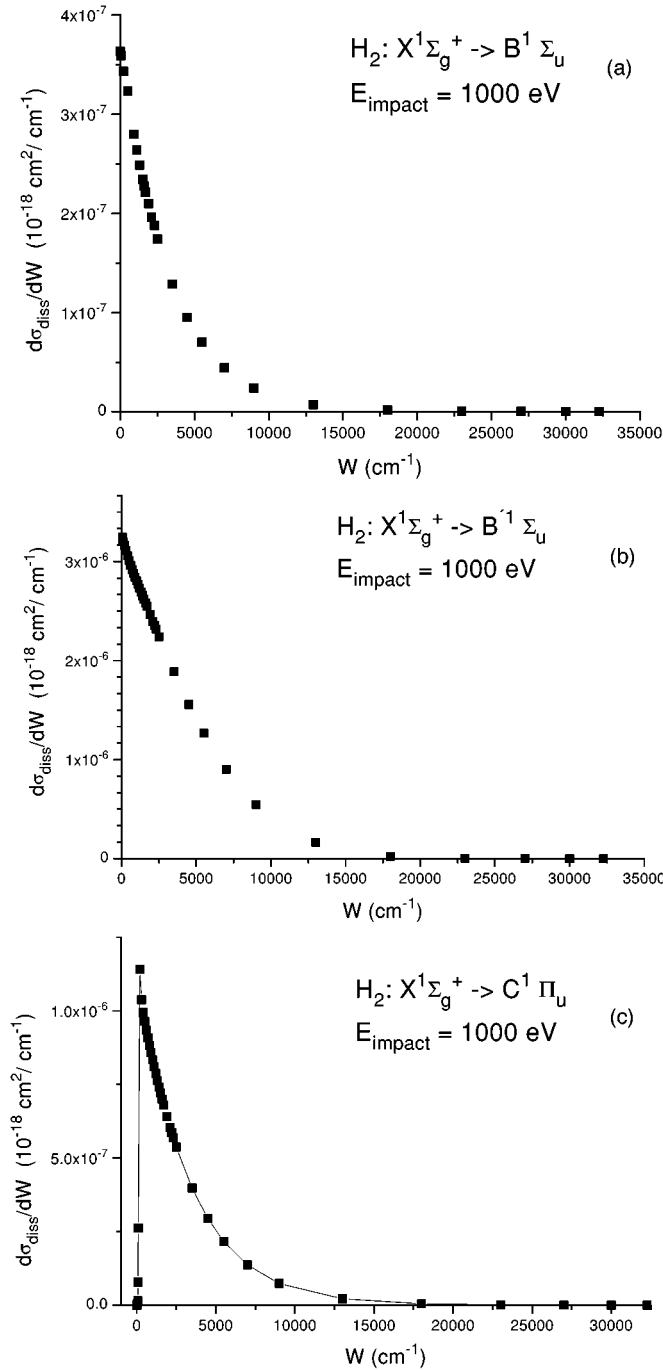


FIG. 2. Dissociation cross sections as a function of the continuum energy W [Eq. (5)] for 1000 eV electron-impact energy for the (a) $X^1\Sigma_g^+(v=0) \rightarrow B^1\Sigma_u^+$, (b) $X^1\Sigma_g^+(v=0) \rightarrow B'^1\Sigma_u^+$, and (c) $X^1\Sigma_g^+ \rightarrow C^1\Pi_u$ transitions.

The differences from the Liu and Hagstrom [4] results range from 27% (100 eV) to 32% (1000 eV), although they have obtained similar dipole transition moments (Table IV) compared to the present results. Probably this difference arises from the utilization of the Bethe approximation [38], which is a further approximation of the first Born approximation valid only at very high electron-impact energies.

Lee *et al.*'s [9] distorted-wave dissociation cross section at 100 eV electron-impact energy has an average difference of 37% from our result. The Born-Ockhur cross sections of

Chung *et al.* [8] have an average difference from our results ranging from 28% (100 eV) to 35% (1000 eV). Both calculations use Hartree-Fock target electronic wave functions and Franck-Condon factors from Spindler [37]. To check for a possible source of this difference, we have calculated the electronic dipole transition moment [Eq. (9)] at $R=1.4$ a.u., using Lee *et al.*'s [9] target wave functions. They have done a Hartree-Fock calculation with improved virtual orbitals [25] to represent the excited state expanded on the Gaussian-type basis set $(10s,7p)/(7s,7p)$. We have obtained for the electronic dipole transition moment, using Lee *et al.*'s [9] wave functions, the value 0.5152 a.u., to be compared with our CI-R value of 0.3886 a.u. and the “exact” result [28] of 0.3996 a.u., as shown in Table III. The average difference between our electronic dipole transition moment and the one obtained from Lee *et al.*'s [9] wave functions is 28%, and the same trend is expected for the dissociation cross sections. A similar behavior is expected for the Born dissociation cross sections of Chung *et al.* [8], which also uses Hartree-Fock wave functions but with a smaller Gaussian basis set $(6s,4p)$. This seems to be the most important factor of the higher cross sections obtained in these works, but the other possible source of discrepancy with Lee *et al.* [9] may be the approximate procedure (Spindler's Franck-Condon factors) in their treatment of the vibrational problem or the utilization of the first Born approximation for 100 eV electron-impact energy in our work.

C. Comparison with experiments

In order to compare our calculations with available experimental results, obtained by detection of the Lyman- α $2p \rightarrow 1s$ transition, we decomposed the available total dissociation cross-section measurements according to Ajello *et al.* [3]. They estimate from electron-impact experiments at 100 eV impact energy that production of $H(2p)$ via direct dissociation of the $B+C$ states accounts for 8.09% of the total dissociation cross sections for producing $H(2p)$. The production of $H(2s)$ via direct dissociation of the B' state accounts for 37.9% of the total dissociation cross sections for producing $H(2s)$. The $H(2s)$ fragments are measured by detecting the Lyman- α from $H(2p)$ obtained by electric field quenching inducing the $2s \rightarrow 2p$ transition. In the following analysis we have considered the decomposition also for higher impact energies, although cascade effects (negligible at 100 eV [3]) and other effects may introduce some uncertainty in this assumption. We cannot estimate the error introduced by this assumption.

The earlier measurements of de Heer and collaborators [6,7] for Lyman- α production of $H(2p)$ are too large by 31% due to a reevaluation of Lyman- α emission by Ajello and collaborators [39]. For this reason, the experimental total dissociation cross sections for production of $H(2p)$ and $H(2s)$ of de Heer and collaborators [6,7] are accordingly reduced by 31% in Figs. 3 and 4. We assume that the errors in the total cross-section measurements are the same in the decomposed cross sections, thus neglecting propagation of errors in the separation of the dissociation channels.

Figure 3 shows our calculations and the experimental results, the latter decomposed according to Ajello *et al.* [3], for production of $H(2p)$ via direct dissociation of the $B+C$

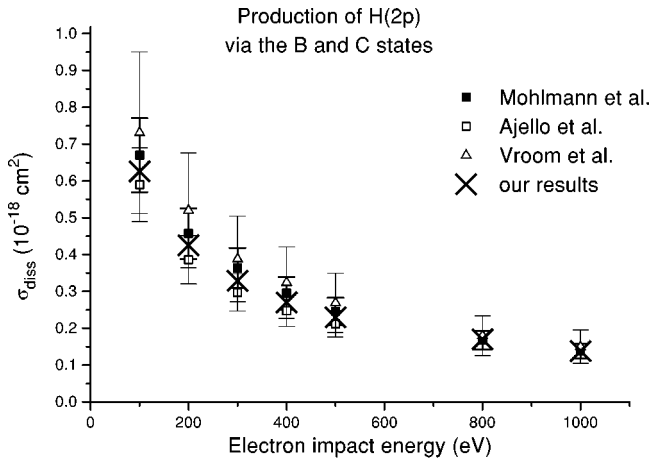


FIG. 3. Our calculated dissociation cross sections [the sum of the values for the B and C states (Tables V and VII) for each electron-impact energy] and the experimental results, the latter decomposed according to Ajello *et al.* [3] and corrected for Lyman- α emission (see text), for production of $H(2p)$ via direct dissociation of the $B+C$ states.

states. The experimental data of Vroom and de Heer [6], besides the Lyman- α correction, are reported with 30% error bars, the Ajello *et al.* have 17% errors bars, and Mohlmann *et al.* have 15%, as estimated from their earlier work [4,41]. The results of Ajello *et al.* [3] are smoothed by a semiempirical model [39,40], which is an extension of the Fano plot [18] to include effects besides the dipole approximation. Our results, the sum of dissociation cross sections for the B and C states (Tables V and VII) for each electron-impact energy, are within experimental error bars. It is worth mentioning the especially good agreement between our calculations and experimental results at 800 and 1000 eV impact energies, well into the region of validity of the first Born approximation.

In Fig. 4 our results are depicted (Table VI) and the experimental results decomposed according to Ajello *et al.* [3] for production of $H(2s)$ via direct dissociation of the B' state. As the photodissociation experiments of Glass-

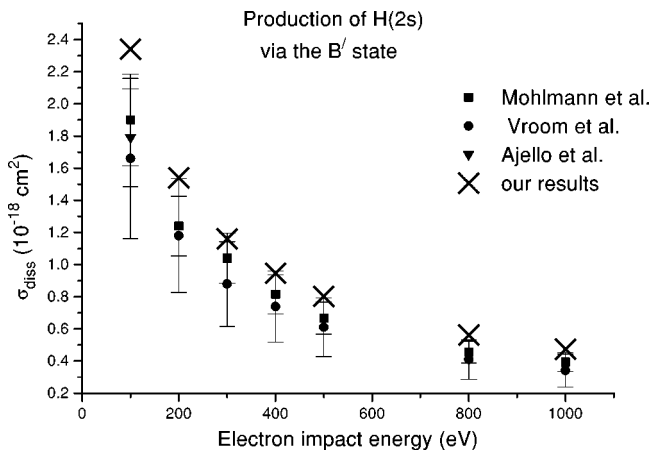


FIG. 4. Our calculated dissociation cross sections and the experimental results, the latter decomposed according to Ajello *et al.* [3] and corrected for Lyman- α emission (see text), for production of $H(2s)$ via direct dissociation of the B' state.

Maujean *et al.* [34] and electron-impact experiments of Ajello *et al.* have shown, the direct dissociation of the B' state is not the major channel of production of $H(2s)$ but accounts only for 37.9% of the total cross section, and other processes take the remaining. Chung, Lin, and Lee [8] erroneously asserted that the B' state would be the main channel (over 95%) for producing $H(2s)$ and Liu and Hagstrom [4] took that for granted. Both assumed that their fair agreement with experimental data confirmed that. Their theoretical dissociation cross sections are overestimated in comparison with our results, as we have shown in the last section. The decomposed experimental cross sections according to Ajello *et al.* [3] confirm this interpretation.

We see in Fig. 4 that our cross sections for direct dissociation via the B' producing $H(2s)$ are somewhat larger than the error bars. In the most favorable experiment [6], the 300 eV impact energy dissociation cross section was 3.1% within the error bar. In the same experiment the other average differences were, above the top of the error bar, 6.9% (100 eV), 7.7% (200 eV), 0.96% (400 eV), 4.5% (500 eV), 7.1% (800 eV), and 4.3% (1000 eV). Contrary to the production of $H(2p)$ fragments, the agreement is not as good as between our calculations and the decomposed experimental results. A possible reason for that may be raised. Experimentally, the metastable $H(2s)$ are made to radiate by application of an electrostatic field across the observation region and measuring the increase in the Lyman- α radiation [6]. This method of electric field quenching (Stark quenching) has been used in all experiments cited here. However, Glass-Maujean shows experimentally [5] that not all $H(2s)$ produced are allowed to emit Lyman- α by electric field quenching but may be destroyed by a nonradiative process forming H_3^+ induced by residual H_2 in the gas chamber, $H(2s) + H_2 \rightarrow H_3^+ + e^-$. This may cause a loss of $H(2s)$ signal produced through direct dissociation by the B' and as a consequence an underestimation of the experimental total dissociation cross sections for producing $H(2s)$. The degree of underestimation cannot be calculated without a great uncertainty, as Glass-Maujean [5] reports.

Other reasons may exist for the discrepancy between experiment and theory for the production of $H(2s)$ through B' . New experiments and decompositions of each of the possible branches of production of $H(2s)$ are thus urgently needed as well other experiments studying the production of $H(2p)$.

IV. CONCLUSIONS

We have computed dissociation cross sections of H_2 for high-energy electron impact (100–1000 eV) producing $H(1s)$, $H(2s)$, and $H(2p)$ from the ground vibrational state ($v=0$) to the continuum of the $B\ ^1\Sigma_u^+$, $B'\ ^1\Sigma_u^+$, and $C\ ^1\Pi_u$ states in the first Born approximation. We have shown that relaxation effects were not important for the calculation of the dissociation cross sections obtained with configuration-interaction electronic wave functions. The Franck-Condon approximation was shown to overestimate the dissociation cross sections, being an especially poor approximation for the dissociation via the $B\ ^1\Sigma_u^+$ and $C\ ^1\Pi_u$ states.

The comparison to experimental results was done using the suggested decomposition of the available total dissociation cross sections measurements according to Ajello *et al.*

[3]. The agreement between the computed dissociation cross sections to produce $H(2p)$ fragments, which is the sum of the dissociation cross sections of the $B\ ^1\Sigma_u^+$ and $C\ ^1\Pi_u$ states and the decomposed experimental results, was very good. On the other hand, the computed cross sections to produce $H(2s)$ fragments, which are related to the dissociation cross section of the $B'\ ^1\Sigma_u^+$ state, were in most cases somewhat larger than the reported experimental error bars. A possible experimental reason for this discrepancy would be that some $H(2s)$ fragments produced by dissociation might be destroyed by a nonradiative process forming H_3^+ induced by residual H_2 in the gas chamber [5]. As a consequence an underestimation of the experimental total dissociation cross sections for producing $H(2s)$ via $B'\ ^1\Sigma_u^+$ might occur.

The good agreement between our computed dissociation cross sections and the decomposed experimental results is very encouraging. We are now applying the methodology presented in this paper to other diatomic molecules. It would be very interesting to perform new experiments not just for the hydrogen molecule but for other diatomic molecules as well.

ACKNOWLEDGMENTS

We thank Professor R. J. Le Roy for providing us with the computer program to obtain the vibrational wave functions and perform the R integration, and Andre G. H. Barbosa for interesting discussions. This work was partially supported by FINEP and CNPq.

-
- [1] N. V. de Castro Faria, I. Borges, Jr., L. F. S. Coelho, and Ginette Jalbert, *Phys. Rev. A* **51**, 3831 (1995); L. F. S. Coelho, Ginette Jalbert, I. Borges, Jr., and N. V. de Castro Faria, *J. Phys. B* **29**, 733 (1996).
- [2] H. Tawara, Y. Itikawa, H. Nishimura, and M. Yoshino, *J. Phys. Chem. Ref. Data* **19**, 617 (1990).
- [3] J. M. Ajello, D. E. Shemansky, and G. K. James, *Astrophys. J.* **371**, 422 (1991).
- [4] J. W. Liu, and S. Hagstrom, *Phys. Rev. A* **50**, 3181 (1994).
- [5] M. Glass-Maujean, *Phys. Rev. Lett.* **62**, 144 (1989).
- [6] A. de Vroom and F. J. de Heer, *Chem. Phys.* **50**, 580 (1969).
- [7] S. R. Mohlmann, K. H. Shima, and F. J. de Heer, *Chem. Phys.* **28**, 331 (1978).
- [8] S. Chung, C. C. Lin, and E. T. P. Lee, *Phys. Rev. A* **12**, 1340 (1975).
- [9] Lee Mu-Tao, R. R. Lucchese, and V. McKoy, *Phys. Rev. A* **26**, 3240 (1982).
- [10] M. J. Redmon, B. C. Garret, L. T. Redmon, and C. W. McCurdy, *Phys. Rev. A* **32**, 3354 (1985).
- [11] R. Celiberto, U. T. Lamanna, and M. Capitelli, *Phys. Rev. A* **50**, 4778 (1994).
- [12] C. E. Bielschowsky, M. A. C. Nascimento, and E. Hollauer, *Phys. Rev. A* **45**, 7942 (1992); M. P. de Miranda, C. E. Bielschowsky, H. M. Boechat Roberty, and G. G. B. de Souza, *Phys. Rev. A* **49**, 2399 (1994); M. P. de Miranda, C. E. Bielschowsky, and M. A. C. Nascimento, *J. Phys. B* **28**, L15 (1995);
- [13] L. M. M. Albuquerque and C. E. Bielschowsky, *Phys. Rev. A* **56**, 2720 (1997).
- [14] C. E. Bielschowsky, C. A. Lucas, G. G. B. de Souza, and J. C. Nogueira, *Phys. Rev. A* **43**, 5975 (1991).
- [15] C. E. Bielschowsky, M. A. C. Nascimento, and E. Hollauer, *J. Phys. B* **23**, L787 (1990).
- [16] C. E. Bielschowsky, M. A. C. Nascimento, and E. Hollauer, *Phys. Rev. A* **42**, 5223 (1990).
- [17] R. Schinke, *Photodissociation Dynamics* (Cambridge University Press, Cambridge, 1993), Chap. 1.
- [18] M. Inokuti, *Rev. Mod. Phys.* **43**, 297 (1971); M. Inokuti, Y. Itikawa, and J. E. Turner, *ibid.* **50**, 23 (1978).
- [19] H. A. Bethe and R. Jackiw, *Intermediate Quantum Mechanics*, 3rd ed. (Benjamin-Cummings Publishing Co., Reading, MA, 1986), Chap. 17.
- [20] S. Chung and C. C. Lin, *Phys. Rev. A* **17**, 1874 (1978).
- [21] R. J. Le Roy, *Comput. Phys. Commun.* **52**, 383 (1989).
- [22] W. Kolos, K. Szalewicz and H. J. Monkhorst, *J. Chem. Phys.* **84**, 3278 (1986); W. Kolos and J. Rychlewski, *ibid.* **98**, 3960 (1993).
- [23] L. Wolniewicz and K. Dressler, *J. Chem. Phys.* **88**, 3861 (1988).
- [24] M. Jaszunski and B. O. Roos, *Mol. Phys.* **52**, 1209 (1984).
- [25] W. J. Hunt and W. A. Goddard III, *Chem. Phys. Lett.* **3**, 414 (1969).
- [26] J. R. Sabin and J. Oddershede, *Nucl. Instrum. Methods Phys. Res. B* **115**, 79 (1996).
- [27] L. Wolniewicz, *J. Chem. Phys.* **51**, 5002 (1969); K. Dressler, and L. Wolniewicz, *ibid.* **82**, 4270 (1985).
- [28] L. Wolniewicz, *Chem. Phys. Lett.* **31**, 248 (1975).
- [29] L. Wolniewicz, *Chem. Phys. Lett.* **233**, 644 (1995).
- [30] A. L. Ford, J. C. Browne, E. J. Shipsey, and P. deVries, *J. Chem. Phys.* **63**, 362 (1975).
- [31] R. Celiberto and T. N. Rescigno, *Phys. Rev. A* **47**, 1939 (1993).
- [32] R. J. Le Roy, R. G. Macdonald, and G. Burns, *J. Chem. Phys.* **65**, 1485 (1976).
- [33] J. A. Beswick and M. Glass-Maujean, *Phys. Rev. A* **35**, 3339 (1987).
- [34] M. Glass-Maujean, P. M. Guyon, and J. Breton, *Phys. Rev. A* **33**, 346 (1986).
- [35] M. Glass-Maujean, *Phys. Rev. A* **33**, 342 (1986).
- [36] I. Dabrowski and G. Herzberg, *Can. J. Phys.* **52**, 1110 (1974).
- [37] R. J. Spindler, *J. Quant. Spectrosc. Radiat. Transf.* **9**, 1041 (1969).
- [38] M. R. C. McDowell and J. P. Coleman, *Introduction to the Theory of Ion-Atom Collisions* (North-Holland Publishing Co., Amsterdam, 1970), Chap. 7.
- [39] D. E. Shemansky, J. M. Ajello, and D. T. Hall, *Astrophys. J.* **296**, 765 (1985).
- [40] D. E. Shemansky, J. M. Ajello, D. T. Hall, and B. Franklin, *Astrophys. J.* **296**, 774 (1985).
- [41] S. R. Mohlmann, F. J. de Heer, and J. Los, *Chem. Phys.* **25**, 103 (1977).